SLAC-R-722

A Study of Proton Production From Energy Ordered Jets Near 10 GeV Center of Mass Energy*

Charles Pearsall

Stanford Linear Accelerator Center
Stanford University
Stanford, CA 94309

SLAC-Report-722
August 2003

Prepared for the Department of Energy
under contract number DE-AC03-76SF00515

Printed in the United States of America. Available from the National Technical Information Service, U.S. Department of Commerce, 5285 Port Royal Road, Springfield, VA 22161.

* M.S. thesis, University of Louisville, Kentucky

A STUDY OF PROTON PRODUCTION FROM ENERGY ORDERED JETS NEAR 10 GeV CENTER OF MASS ENERGY

By

Charles Pearsall
B.S., University of Louisville, 2001

A Thesis
Submitted to the Faculty of the
Graduate School of the University of Louisville
in Partial Fulfillment of the Requirements
for the Degree of

Master of Science

Department of Physics
University of Louisville
Louisville, Kentucky

August 2003

A STUDY OF PROTON PRODUCTION FROM ENERGY ORDERED JETS NEAR 10 GeV CENTER OF MASS ENERGY

By

Charles Pearsall
B.S., University of Louisville, 2001

A Thesis Approved On

Date

by the following Thesis Committee:

Thesis Director

ACKNOWLEDGEMENTS

I would like to express my gratitude to all those that gave me the opportunity to complete this thesis. This work would not have been possible without the guidance, instruction, patience, and encouragement of my adviser Dr. David N. Brown. His help was invaluable and the example he set for me has had a great impact on my edcuation. I would also like to thank my wife, Danna for her extreme patience and unwavering support for me. Thanks also go out to Dr. Joseph Chalmers and Dr. Lee Larson for agreeing to serve on my thesis committee. I am grateful to the HEP group members for their help and valuable comments.

This work is supported in part by U.S. Department of Energy Grant DE-FG02-98ER41089.

ABSTRACT

A STUDY OF PROTON PRODUCTION FROM ENERGY ORDERED JETS NEAR 10 GeV CENTER OF MASS ENERGY

Charles Pearsall

August 6, 2003

We investigate hadronic jets ordered by energy from e^+e^- annihilations near 10 GeV center of mass energy. The fraction of protons produced from both two jet and three jet events are measured using jet finding software. We find the average ratio of protons in lowest energy jets compared to the average of the two highest energy jets to be $1.3705 \pm 0.0298 \pm 0.0260$ where the first error is systematic and the second is statistical. This work is performed with the *BaBar* detector at the Stanford Linear Accelerator Center (SLAC).

TABLE OF CONTENTS

LIST OF TABLES

LIST OF FIGURES

CHAPTER I

INTRODUCTION

A The Standard Model

The Standard Model (SM) is the current theory that describes particles and fundamental interactions. First developed in the 1970's, the SM summarizes the current knowledge of particle physics. The Standard Model is a quantum theory combining electroweak theory, or Quantum Electrodynamics (QED) and the theory of strong interactions, or Quantum Chromodynamics (QCD) [1]. According to this model, all matter is primarily made of a small number of fundamental particles. This model has successfully predicted several particles that were later found by experiment and describes a significant amount about the universe and interactions correctly. Despite the successes of the Standard Model, it is unlikely to be the final theory of particles and interactions. It has several limitations including its failure to incorporate a theory of quantum gravity, the mass of neutrinos, a large matter-antimatter asymmetry, and that 96% of the apparent mass of the universe is not visible [1].

Particles are divided into two groups, fermions and bosons. Fermions comprise nearly all visible matter and have $\frac{1}{2}$ integer spin. They follow Fermi-Dirac spin statistics; therefore they are antisymmetric under exchange of identical fermions. Bosons have integral spin and follow Bose-Einstein statistics; therefore they are symmetric under exchange of identical bosons [1].

For every particle there is an antiparticle that has the same mass, spin, and lifetime, but that has opposite electric charge and magnetic moment. Several

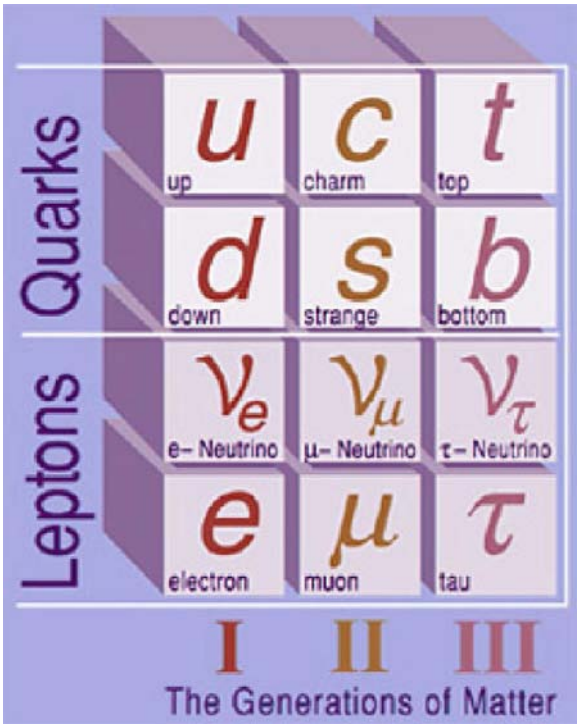

Figure 1. Quarks and leptons divided by generation. Image courtesy of Fermi National Accelerator Laboratory.

electrically neutral particles are their own antiparticle [1].

The fermions are divided into two groups of fundamental particles, leptons and quarks. Quarks and leptons divided by generation are shown in Figure 1.

B Fundamental Particles

1 Leptons

Leptons carry integral charge and include the electron (e), muon (μ), tau particle (τ), neutrinos (ν_e, ν_μ, ν_τ) and their associated antiparticles. Each different lepton is referred to as a particular "flavor." Leptons are further divided into three generations of a charged lepton and its associated neutrino. Including the antiparticles, there are twelve fundamental leptons.

Leptons carry integral electric charge. The three charge -1 leptons are the electron ($m_e = .511$ MeV), the muon ($m_\mu = 105.66$ MeV), and the tau particle ($m_\tau = 1776.99$ MeV) [2]. The three charge 0 leptons are called neutrinos, each associated with a charged lepton. These pairs of charged and neutral leptons form the generations.

The electron is the most familiar of the leptons, has a negative charge, and is very light in mass as compared to nucleons. The electron neutrino (ν_e) was first theorized by Pauli in nuclear β decay in 1930. This process was observed at the base level to be

$$n \rightarrow p + e^-.$$

There is missing momentum from the observed final states that violates the long-held Law of Conservation of Momentum. Pauli concluded that there must be a missing particle he dubbed the neutrino to account for the lost momentum. The neutrino was not experimentally discovered until 1956 [1].

The μ and the τ are unstable heavy charged leptons similar to the electron. The μ was first discovered in cosmic rays in 1937 and the τ was observed in 1975 at the Stanford Linear Accelerator Center (SLAC). Neutrinos are assumed to have zero mass by the Standard Model, but there is significant evidence that they have non-zero mass [1]. Figure 2 shows a list of leptons and their properties.

2 Quarks

Quarks are divided into three generations according to mass. Each generation contains one positively charged and one negatively charged quark. The quark flavors include the up, down, strange, charm, bottom, and top. Similarly, there are twelve quarks including the antiparticles. Quarks have the interesting property of only existing in combinations, never individually. Particles containing quarks are called hadrons. These hadrons occur as a quark-antiquark pair, called a meson, or a set of three quarks called a baryon. Quarks are required by the Pauli-exclusion principle

	Flavor	Mass (GeV/c^2)	Elect. Charge
ν_e	e neutrino	$< 7 \times 10^{-9}$	0
e^-	electron	.000511	-1
ν_μ	μ neutrino	< .0003	0
μ^-	muon	0.106	-1
ν_τ	τ neutrino	< .03	0
τ^-	tau	1.7771	-1

Figure 2. Table of lepton mass and charges

to have an additional degree of freedom that is called "color" charge. The Pauli-exclusion principle states that two or more fermions cannot exist in the same quantum state. Due to the color charge of each quark state, the exclusion principle is not violated inside hadrons [1].

Quarks carry fractional charges and have spin $\frac{1}{2}$. The quarks cannot be separated due to the high binding energy holding these particles together, so the individual masses are difficult to distinguish [3]. There are six quark types in three generations. Each generation contains a quark that has an electric charge of $+\frac{2}{3}$ and one of $-\frac{1}{3}$. The antiquarks have electric charges of $-\frac{2}{3}$ and $+\frac{1}{3}$. Each successive generation increases the quark's masses. The first generation of quarks, containing up and down, are the only stable quarks. These particles compose protons (uud) and neutrons (udd). The properties of quarks are displayed in Figure 3.

The up and down quarks constitute nucleons and form the bulk of the visible universe. The strange quark was discovered in the 1950's and was named after the odd properties that particles containing these quarks displayed [4].

The experimental observation that these strange particles were only produced in pairs from non-strange hadrons was the first indication of a new quark. These strange particles, like the $K^{\pm}$ and the $\Sigma^{\pm}$ had extremely long lifetimes as compared

Flavor	Mass(GeV/c²)	Elect. Charge
u up	.005	+2/3
d down	.01	-1/3
c charm	1.5	+2/3
s strange	0.2	-1/3
t top	180	+2/3
b bottom	4.7	-1/3

Figure 3. Table of quark masses and charges

to similarly massive particles like the δ which decayed strongly. From this, a new quantum number was assigned to these particles and it was asserted that this "strangeness" number is conserved in strong and electromagnetic interactions, but can be violated in weak interactions. This assertion explains the strange particle pair production in strong interactions,

$$\pi^+ + p \rightarrow K^+ + \Sigma^+$$

where the Σ^+ and the K^+ are strange particles. The long-lived decay of

$$\Sigma^+ \rightarrow p + \pi^0$$

is explained to be a weak interaction decay of a strange quark [4].

The charm quark was discovered by two independant experiments in 1974. One at SLAC, and the other at Brookhaven, New York. Each place named the particle separately, so it became known by both names, the J/Ψ. The J/Ψ is a meson comprised of a charm quark and a charm antiquark ($c\bar{c}$). The bottom quark was discovered at FermiLab from the detection of the Υ meson ($b\bar{b}$) in 1977. The top quark was not discovered until 1995 at the Tevatron at FermiLab [1].

In the two heavier generations, the quarks are given flavor quantum numbers to show flavor conservation. In strong interactions where these quarks are produced,

the net flavor number must be the same as the initial states. There are flavor changing interactions, but these occur via the weak force [1].

C Fundamental Forces

There are four fundamental interactions in the Standard Model. Each force is mediated by a fundamental particle. The strong force binds quarks together into hadrons and is mediated by the gluon. This force is responsible for quark confinement and asymptotic freedom. The electromagnetic force is either a repulsive or attractive force that effects charged particles. The mediating particle is the photon. The weak interaction is a flavor changing interaction of quarks and leptons. It is mediated by the $W^{\pm}$ and the Z^0. Last is the gravitational interaction, which is by far the weakest force at the energy scales of experimental particle physics, but dominates the scale of the universe. It is mediated by the graviton, a spin 2 boson that is still undiscovered. The properties of the fundamental forces are listed in Table 1 [1].

TABLE 1

The Fundamental Forces. Note that Relative Strength is relative to the EM interaction at a distance of 1 fm, table courtesy of Jianping Pan

FORCE	CARRIER(S)	RELATIVE STRENGTH	RANGE (m)
Strong	Gluons	1	10^{-15}
Electromagnetic	Photon	7×10^{-3}	infinite
Weak	$W^{\pm}, Z^0$	10^{-5}	10^{-17}
Gravitation	Graviton	6×10^{-39}	infinite

The fundamental interactions are most easily described as an exchange of particles. This exchange provides a rate of change of momentum, thus a force is passed. At the fundamental particle scale, these exchange particles are the force carrying bosons. Exchanged particles do not satisfy classical conservation laws.

They are allowed, and limited by, the Uncertainty Principle. This process has to take place within a time Δt with an exchange particle of energy ΔE such that

$$\Delta E \; \Delta t \; \simeq \; \hbar.$$

These types are particles are referred to as virtual particles [1].

These interactions are quantized, meaning that they continually emit and absorb force carrying particles that transfer a multiple of a basic unit of energy. This is different from the classical force field theory, but since neither the field nor the virtual particles can be detected. The force that they apply is the only thing that can be measured directly [1].

1 Electromagnetic Interaction

The electromagnetic interaction is between particles that carry an electric charge. The electric and magnetic fields have vector transformation properties. The photon is the force carrier, is a vector boson, has infinite range because it has zero mass, and it propagates at the speed of light. This propagation is a consequence of relativity, which states that a particle traveling at the speed of light must have zero mass. A quantum effect only seen at the smallest particle scales is virtual particle pairs being created and shortly annihilating. This effect is referred to as "vacuum polarization." Because of the Coulomb field of an electrically charged particle, the vacuum containing pairs of virtual e^+e^- becomes polarized. For the EM interaction, vacuum polarization reduces the charge detected at larger distances. [1].

2 Strong Interaction

The strong interaction of forces between quarks is mediated by the gluon. Quantum Chromodynamics contains six types of strong charge, as opposed to the electromagnetic interaction where there are two types. These six QCD charges are referred to as "color" charges. A quark can carry only one type of color charge:

either red, blue, or green. The antiquark carries the anticolors. QCD is totally color charge symmetric, meaning that no matter what color charge the quark carries, its interactions are the same. Quarks only exist in pairs (mesons) or triplets (baryons)and the net color charge on these particles is always neutral. Mesons are a quark-antiquark pair and the color charge on each is opposite, leaving a net neutral charge. Baryons contain three quarks, each with a different color, also leaving a net neutral color. Gluons carry two color charges, a color and an anticolor. This gives $3 \times 3 = 9$ possible gluons, but only eight exist because of a color singlet state $(r\bar{r} + g\bar{g} + b\bar{b})$ [1].

3 Weak Interaction

The weak interaction takes place between quarks and leptons and are usually dominated by the strong and electromagnetic interactions. Flavor changing interactions are strictly weak. These interaction is mediated by the charged ($W^{\pm}$) and neutral (Z^0) vector bosons. Due to the large mass of the mediators, the relative strength and distance at which the interaction occurs is very small. But, this also give rise to the relatively slow decay process ($\sim 10^{-18}$ seconds).

One example of the weak interaction is muon decay. This is

$$\mu^- \rightarrow \nu_\mu + \nu_e + e^-$$

The weak interaction conserves lepton number, but can violate quark quantum numbers. For example, the weak decay of

$$\Lambda^0 \rightarrow p + \pi^-$$

is a flavor changing reaction. The Λ particle contains a quark structure of uds. The proton consists of uud and the pion $\bar{u}d$. The violation here is the strangeness number violation. At the base quark level, the strange quark (s) decays into a up quark (u) and emits a pion (π^-) to conserve charge [1].

4 Gravitation Interaction

Gravity is the dominating force on the universal scale, but at the subatomic scale it is the weakest interaction. In the Standard Model, gravity is totally neglected. It is mentioned for completeness, but its integration into the Standard Model is one of the major problems in modern High Energy Physics.

D Quantum Chromodynamics

Quantum Chromodynamics is the current theory of the strong interaction. This theory is similar to Quantum Electrodynamics in that it is a renormalizable gauge theory. QCD grew out of the need to solve the Fermi statistics violating Δ^{++} particle which required an additional degree of freedom with a property called "color." It made the theoretical cross-section of $e^+e^- \rightarrow hadrons$ triple and come into agreement with experimental data. In addition, deep inelastic scattering measurements require the existence of electrically neutral and charged constituents of the proton [4]. These are the color carrying gluons, the bosonic force carrier of QCD.

The main properties of QCD include [4]:

- quarks carry both color and electric charge;
- there are three color charges and their anti-colors: red (R), green (G), blue (B), anti-red ($\bar{R}$), anti-green ($\bar{G}$), and anti-blue ($\bar{B}$);
- color is exchanged by gluons;
- there are eight gluons: $R\bar{B}$, $R\bar{G}$, $B\bar{G}$, $B\bar{R}$, $G\bar{R}$, $G\bar{B}$, $\frac{1}{\sqrt{2}}(R\bar{R} - B\bar{B})$, and $\frac{1}{\sqrt{6}}(R\bar{R} + B\bar{B} - 2G\bar{G})$;
- quark-gluon interactions are computed by the rules of QED with the substitution $\sqrt{\alpha} \rightarrow \sqrt{\alpha_s}$ and the introduction of a color factor;

- QCD exhibits asymptotic freedom at short distances and quark confinement at larger distances.

Quarks carry a color charge; either red, blue or green. Anti-quarks carry an anti-color, either anti-red, anti-blue, or anti-green. These are sometimes called cyan, magenta, and yellow, to conform to actual visible color spectrum opposites, but for ease of use, anti-color terminology will be used here. These colors do not refer to an actual electromagnetic spectrum color values, but use the color as an analogy.

Because there are three colors and anti-colors, it would seem that there should be nine color combinations of gluons; however, using group theory we find there are eight real states and one color singlet which is excluded because it carries no net color.

The color charge is similar to electric charge in the Electromagnetic (EM) interaction. The main difference is that the EM interaction has two charges mediated by an uncharged boson (photon), while the strong interaction consists of six color charges and is mediated by a charged boson (gluon). QCD predicts that only two quark configurations exist. They are the QQQ state, which is a baryon, and the $Q\bar{Q}$, which is the meson. Other possible combinations like QQ , $QQ\bar{Q}\bar{Q}$, or $QQQQ$ are repulsive by QCD calculations and do not exist. These predictions have been verified by experiment [1].

The basic form of the QCD potential is

$$V = -\frac{4}{3}\frac{\alpha_s}{r} + kr$$

This is similar to the Coulomb potential, but there are differences with the strong interaction. The main difference is that the α_s term is not a constant. It is called the running coupling constant because the value of the constant depends on the energy scale involved.

At small distances, the strong interaction reduces in magnitude. This is called asymptotic freedom where the quarks and gluons are free to move around within a

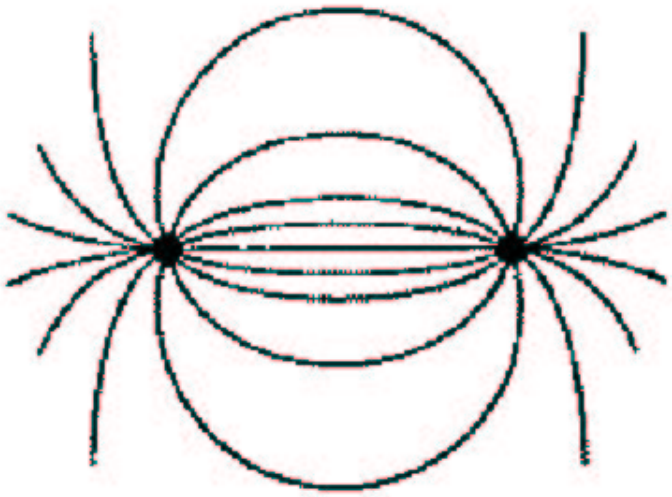

Figure 4. Field lines between electromagnetic charges

limited radius from each other and have minimal attraction. As the distances from each other increase, the attractive forces increase. At greater distances, the quarks are confined, because gluons exchanged between quarks are attracted to each other.

This is best illustrated using the color flux tube model. If self-coupling of gluons is neglected, the color field lines for a pair of quarks would resemble an EM dipole field as shown in Figure 4. QCD states that gluons do interact with each other, and its effects are shown in Figure 5.

In the case where quarks are close together, the color field lines will be further apart from each other and there will be less attractive forces on the quarks. But, as the quarks move further apart, there will be less attractive forces. This is best visualized by imagining the color flux tube is a rubber band. When the particles are close the force is small; but, as the partivles are pulled apart, the attractive forces and total energy increases [4].

At some point, the energy required to move the two quarks further apart is more than the energy to create two more quarks out of energy to mass conversion. At these small distances, time, and energies; mass and energy become

Figure 5. The color field lines of two quarks.

interchangeable by Einstein's $E = mc^2$ equation. Since the universe likes to progress towards a lower energy state, a quark anti-quark pair will be created and each will bind with a preexisting quark into two quark-anti-quark pairs. This process is called fragmentation [4].

E Fragmentation and Jets

Similar to the Electromagnetic interaction, Quantum Chromodynamics has a vacuum polarization process to screen the color charge. In space, electron-positron pairs will spontaneously appear, travel some distance, and then annihilate. This event follows the uncertainty principle,

$$\Delta t \Delta E \simeq \hbar$$

which states that an uncertainty in energy (ΔE) can exist for some lifetime (Δt) as long as the product of the two is less than or equal to $\hbar$. When this occurs near an electric charge, the short lived particles will interact with the charge. The net effect is to shield the charge from outside measurements. If a charge is measured from different distances, the resultant value will increase as you get closer to the charge. This same process occurs with gluons coming in and out of existence for short periods of time. When in proximity to a color-charged object they will anti-shield the color charge. This means that with large color charges (greater distance), the attraction will be spread out over the entire vacuum polarized area and will result in weaker coupling [1].

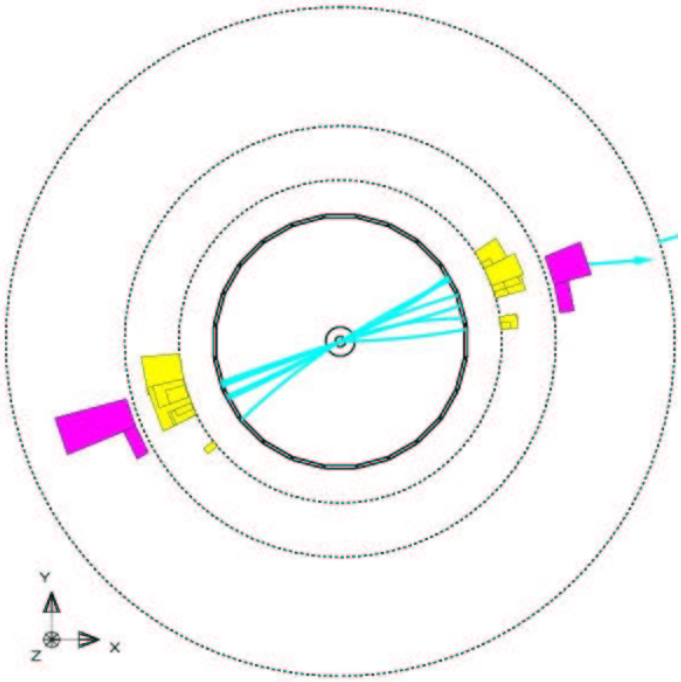

Figure 6. Computer reconstruction of a typical 2 jet event. The lines indicate observed tracks in the drift chamber and the trapezoids indicate energy deposited in the outer detector areas. The interaction point is at the center.

Quark theory predicts that there should be two jets of hadrons from the decay of a virtual photon in opposite directions to conserve momentum. Figure 6 shows a computer reconstruction of a typical two jet event. In a two jet event, two sprays of hadrons should be observed back to back originating from an interaction point. A theory without quarks would expect a uniform, isotropic distribution of hadrons. The experimental result is that of the quark model [4].

A virtual photon decays into a quark anti-quark pair, these quarks separate and momentum conservation requires that they move in opposite directions with equal momentum in the center of mass frame (CM). As the pair get further apart the color field lines get closer together and the force attracting the quarks increases. When the energy contained in the attractive potential reaches the same amount to create another quark anti-quark pair, the pair will be created and then the two

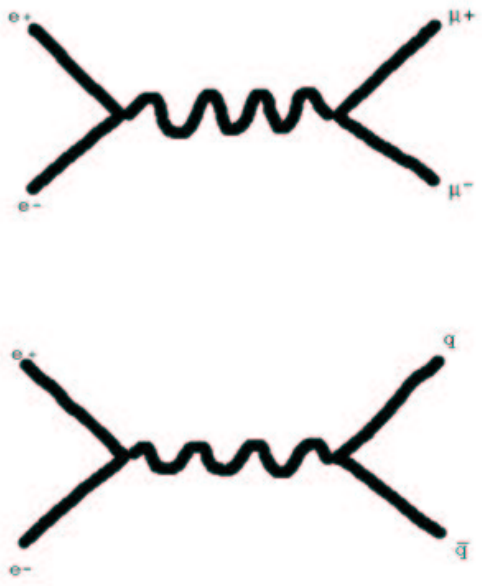

Figure 7. Top Feynman diagram is a typical QED process. Bottom diagram is a typical QCD process.

hadrons move apart back to back as the originators of the jets. These newly created jets will begin to fragment into other hadrons and there will be two sprays of hadrons in a cone surrounding the initial jet orientations.

By examining e^+e^- annihilations into hadrons we can study properties of hadrons and quarks. The lepton collisions provide a clean environment from colliding hadrons in that the lepton collisions are fundamental particles and contain no substructure that we know. Hadrons produced in e^+e^- annihilations are predominantly the daughters of quarks and anti-quarks decaying [4].

The cross-section of $e^+e^- \rightarrow Q\bar{Q}$ can be calculated from a similar QED process $e^+e^- \rightarrow \mu^+\mu-$. The Feynman diagrams for both of these processes are shown in Figure 7. From QED, the cross-section (σ) is

$$\sigma(e^+e^- \rightarrow \mu^+\mu-) = \frac{4\pi\alpha^2}{3Q^2} \text{ [4]}$$

Since the quarks can have three different color charges a factor has to be added to take this multiplicity into account. It is $3q^2$, where q is the charge on the

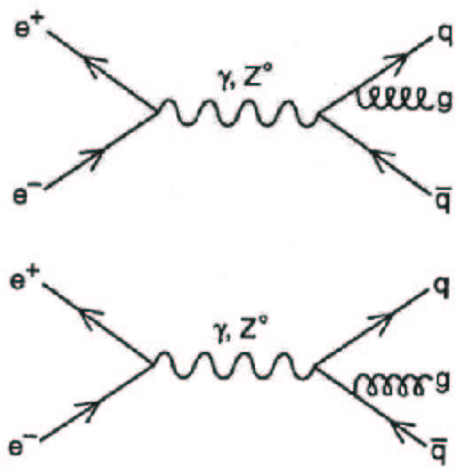

Figure 8. The most common second order processes where either quark can emit a gluon.

quark [4].

These results need to be modified for second order processes. This is where the quark and/or anti-quark radiate gluons. This is of the form $e^+e^- \to Q\bar{Q}G$ The Feynman diagrams of this second order process are shown in Figure 8.

This cross section can be obtained from the cross section of $e^+e^- \to Q\bar{Q}$. Start with the square of the amplitude for the sum of $\gamma^* \to Q\bar{Q}G$, which is

$$\mid \mathcal{M} \mid^2 = N(\frac{t}{s} + \frac{s}{t} + \frac{2uQ^2}{st})$$

where N is the normalization factors and coupling constants and where $s = (p_\gamma - p_q)^2$, $t = (p_\gamma - p_{\bar{q}})^2$, $u = (p_\gamma - p_g)^2$, and $Q^2 \equiv p_\gamma^2$. From this we rewrite the initial equation in terms of the energy fraction variables and obtain

$$\mid \mathcal{M} \mid^2 = N\frac{x_q^2 + x_{\bar{q}}^2}{(1 - x_q)(1 - x_{\bar{q}})}$$

Now we relate this expression to a e^+e^- pair and we get

$$\frac{d\sigma}{dx_q dx_{\bar{q}}} = N'\frac{x_q^2 + x_{\bar{q}}^2}{(1 - x_q)(1 - x_{\bar{q}})}$$

[4].

Then following the procedure outlined in Halzen and Martin's *Quarks and Leptons* we get the exact $\mathcal{O}(\alpha_s)$ result becomes

$$\frac{1}{\sigma}\frac{d\sigma}{dx_q dx_{\bar{q}}} = \frac{2\alpha_s}{3\pi}\frac{x_q^2 + 2_{\bar{q}}^2}{(1-x_q)(1-x_{\bar{q}})}$$

where the renormalization coefficient N' is

$$N' = \frac{2\alpha_s}{3\pi}\sigma \ [4]$$

This leads to the QCD prediction of the angular distribution of jets. The distribution can be written as

$$\frac{1}{\sigma}\frac{d\sigma}{dp_T^2} \sim \alpha_s \frac{1}{p_T^2}\log(\frac{Q^2}{4p_T^2})$$

where p_T^2 is the transverse momentum between the quark-antiquark as a result of the emission of the gluon.

From these a prediction of the cone width of a fragmented jet can be found. At high energies QCD predicts

$$< \theta > \simeq \frac{< k_T >}{p_q}$$

This also applies to a gluon fragmentation. [4] Gluon fragmentation occurs when one of the initial pair of quark-antiquark emits a gluon before fragmenting into other hadrons. This gluon decays into a quark-antiquark pair and these continue with fragmentation. The detected result of this emitted gluon is called a three jet event and is pictured in Figure 9 [4].

Many experiments have studied particle production in e^+e^- events and looked at differences between quark and gluon jet fragmentation. Most of the differences noted thus far are in general jet characteristics such as angular spread, transverse momentum, and overall particle multiplicity. Gluon jets are found to have a greater angular spread, more momentum transverse to the jet axis, and a higher overall particle multiplicity. These findings are in agreement with QCD

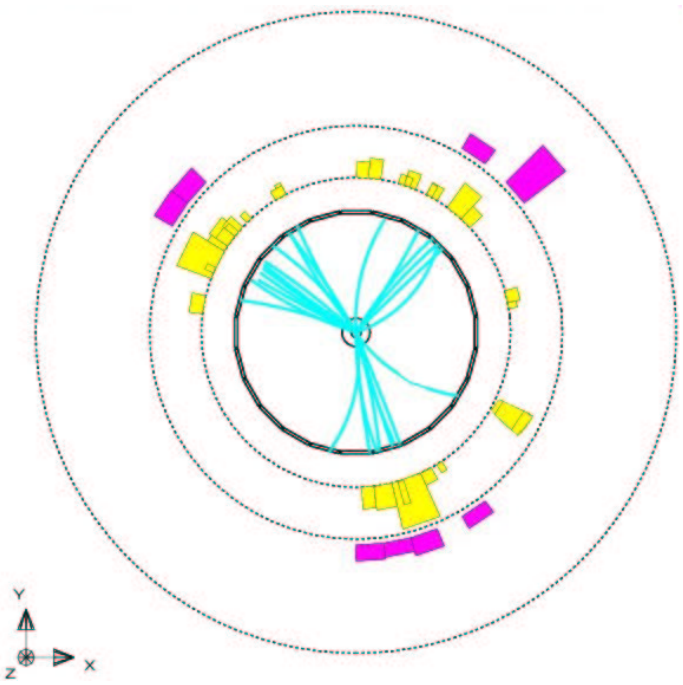

Figure 9. Computer reconstruction of a typical 3 jet event.

qualitatively, but QCD predicts no actual difference between the fragmentation products of a gluon jet versus and quark jet [5]. The multiplicity of p and Λ particles in events dominated by gluon fragmentation have been measured to be higher than statistical errors. The ratio of overall charged particle multiplicity in $e^+e^- \to \Upsilon(1S) \to ggg \to$ hadrons to that in $e^+e^- \to q\bar{q}$ is approximately 1.3 while the ratio for baryon multiplicity is approximately 2.5 [5].

This issue has been disregarded with the reasoning that it is a byproduct of event topology or final state interactions. However, a study by Dr. David N. Brown at CLEO showed that baryon production increases with increasing sphericity in continuum events while the production decreases with increasing sphericity in $\Upsilon(1S) \to ggg$ events [5]. This suggests that "baryon enhancement" is an energy-dependent property of individual gluon jets.

In this thesis, we will utilize the fact that protons can be easily identified in

large numbers at the *BaBar* detector and they will be the target of study to test individual gluon jets for a possible source of new information on QCD. The large continuum data sets available, coupled with excellent vertex separation, will allow the first baryon production survey that can be directly pinned to gluons through jet-finding analyses. We will make a direct determination of proton multiplicities per jet that we order by energy [5].

CHAPTER II

THE BABAR EXPERIMENT

The *BaBar* detector is situated on the PEP-II B Factory which uses the linear accelerator at SLAC as the injector. The primary goal of the *BaBar* experiment is the study of CP asymmetries in the decays of neutral B mesons. A detailed and systematic study of this would also yield a measurement of V_{ub}, a Cabbibo-Kobayashi-Maskawa (CKM) matrix element, measure a number of rare B meson decays, and help to put good constraints on the parameters of the Standard Model [6].

A Stanford Linear Accelerator Center

SLAC is one of the world's leading research laboratories. Established in 1962, it is located at Stanford University in Menlo Park, CA. It was created to establish an electron accelerator and related facilities and be used for high-energy physics and synchrotron radiation research. Figure 10 gives an overhead drawing of the accelerator and collision rings at SLAC. Three Nobel prizes have been awarded to scientists working at SLAC.

Burton Richter of SLAC received the Nobel prize in physics along with Samuel Ting of MIT for the discovery of the charm quark in 1974. Richard Taylor of SLAC received the Nobel prize along with Henry Kendall and Jerome Friedman of MIT for deep inelastic scattering experiments in 1990. Most recently, Martin Perl of SLAC and Frederick Reines of UC Irvine received the Nobel prize for the discovery of the τ particle [7].

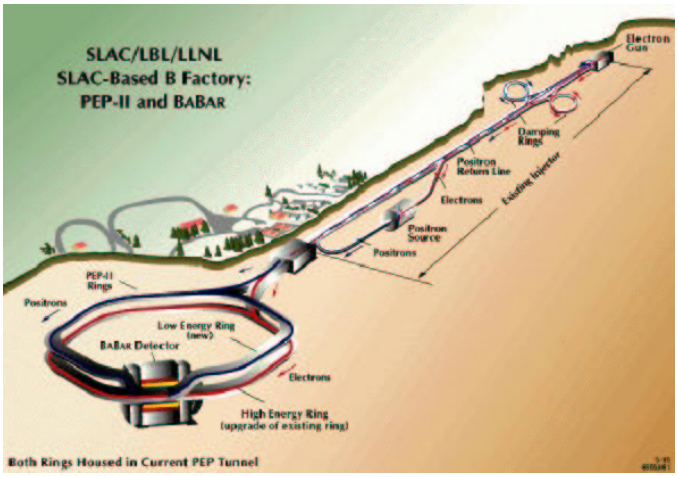

Figure 10. View of the Stanford Linear Accelerator Center

The current accelerator at SLAC is a two mile long linear accelerator. It is powered by klystrons to provide an electromagnetic wave to accelerate the electrons and positrons along the length. At the end of the two mile long stretch, the electrons and positrons are divided into two different sets of rings, called the PEP-II. These are a pair of storage rings for the electrons and positrons until they are collided inside a detector [7].

PEP-II provides the best source of neutral B mesons the use in the *BaBar* detector. It consists of an e^+e^- asymmetric colliding beam. This operates at the $\Upsilon(4S)$ resonance, which is the first particle with enough energy to create a $b\bar{b}$ system. Since most of the energy from the annihilation reaction goes into creating the B^0 meson, there is very little energy left over to be momentum. This leaves the particle nearly at rest in the center of mass frame and allows for a high precision measurement of the decay time. The lepton collider was chosen over a hadron collider due to several considerations, including a high signal to noise ratio, clean events with an average of 11 charged particles, and low interaction rates [6].

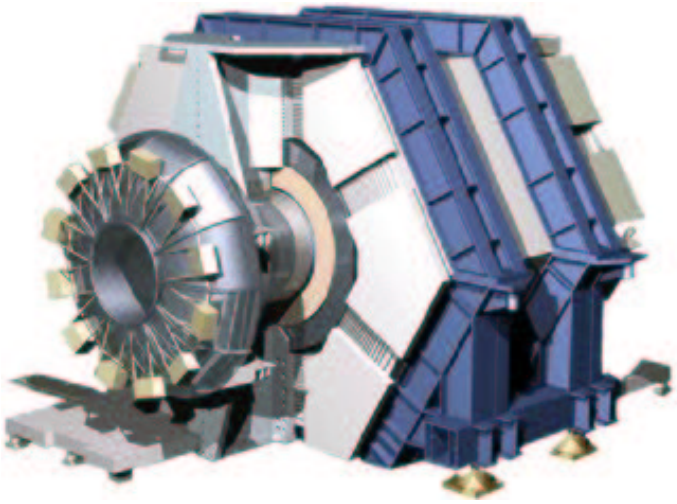

Figure 11. The BaBar detector

B BaBar Detector

The *BaBar* detector was designed with a set of design goals. It is pictured in Figure 11. One goal is to have the largest possible acceptance in the center of mass system. The colliding beams are asymmetric and so the detector needs to also be asymmetric. Another goal is to have detectors as close as possible to the interaction region. Excellent vertex resolution is needed because B mesons will travel very close to the z-axis, so high z-component detector resolution is needed while minimizing multiple scattering. In addition, the detector needs a range of 60 MeV to 4 GeV transverse momentum and have high efficiency flavor tagging. The detector also needs a large photon and neutral pion energy range and the ability to detect neutral hadrons. The *BaBar* detector was designed to include all these parameters [6].

1 Silicon Vertex Tracker

The silicon vertex tracker primarily measures the z separation between the two B mesons. It can resolve to within 70 microns within its confines. As the innermost detector, the SVT provides the best angular measurement and detects

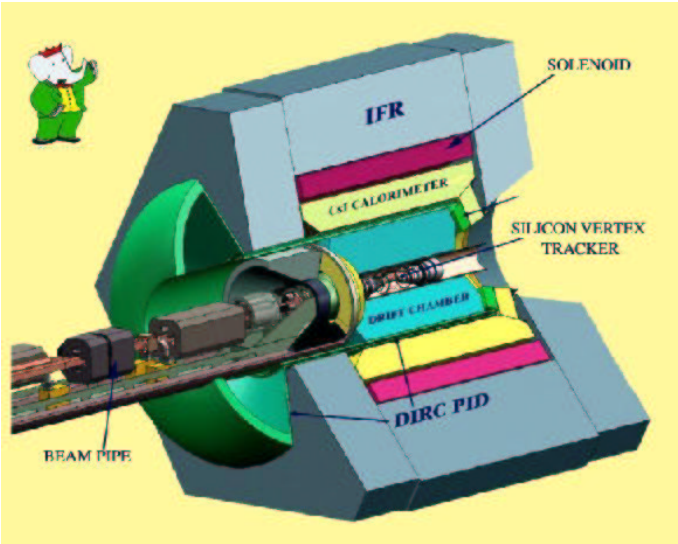

Figure 12. Components of the BaBar detector

low momentum particles that will not pass completely through into the drift chamber. It can discriminate between beam annihilations and short lived particles decay products. Charm and bottom quark containing mesons are detected here [8].

The SVT consists of five concentric cylinders and covers a maximum polar angles between 20.1 deg and 150.2 deg. The inner three layers each contain six modules arranged in a hexagonal structure that has a slight overlap. The two outer layers consist of 16 and 18 detector modules and are arranged in an arch. Each module is double sided and contains a silicon microstrip detector [6].

2 Drift Chamber

The drift chamber is the main tracking device of the *BaBar* detector and it gives very high reconstruction efficiencies for tracks. This component along with the SVT provide excellent position and momentum resolution needed for the reconstruction of events. The drift chamber is cylindrical in shape, and has the impact point off center due to the asymmetric nature of the beams. The drift cells

consist of 10 layers of which each layer is subdivided into four more layers. The main layers alternate using axial alignment and two different stereo alignments. The cells of each layer consist of gold-plated tungsten-rhenium wires arranged either in a stereo configuration or axially and are at approximately 2000 Volts. The whole assembly is contained in a 1.5 Tesla magnetic field used to detect charges on particles. The electronics were designed to keep up with the performance of the detection rates and act as one of the triggering mechanisms [6].

3 DIRC

The DIRC or detection of internally reflected Cherenkov light is designed for particle identification. It uses long bars of quartz to bring the Cherenkov light outside the main structure to the light detector. It does this through a series of internal reflections in the quartz. At the end of the quartz bars the light that retains its initial angle enters a Standoff Box filled with water and containing the photomultiplier tubes. The DIRC consists of 144 bars of rectangular quartz arranged in a 12 sided shape around the beam cylinder. This design leaves about 8 cm of radial space, directly around the main detector tunnel to allow for other instrumentation. The DIRC provides excellent mass discrimination for each of the five charged particle possibilities (e, μ, π, K, and p) [6].

4 The Electromagnetic Calorimeter

The Electromagnetic Calorimeter (EMC) is designed to detect both charged and neutral particles. The amount of charge deposited in the calorimeter in a single shower and the depth to which the shower develops are proportional to the total energy of the particle that initiated the shower. The showers from charged particles are identified by the relationship between the location of the shower and the direction of a track seen in the inner layers. A shower that has no associated track tells us about a neutral particle that was produced in the event [8].

The EMC is made of cesium-iodide crystals read out by photodiodes. It is shaped of a cylindrical barrel section with a forward conic endcap and consists of 5760 crystals arranged in 48 rows. The EMC does not give total coverage due to having to stay away from the forward and backward edges to avoid shower leakage [6].

5 Instrumented Flux Return

This part of the *BaBar* detector is mainly a muon and neutral hadron detector. Most particles produced in the collisions are stopped in the calorimeter. Only the most energetic hadron showers, muons, and neutrinos penetrate into this last set of layers. The neutrinos will pass through this layer without interacting. Neutrinos can only be found by the inference of missing energy and momentum from an event. They rarely interact with matter. The IFR consists of a central barrel and two end caps each made of layers of iron plates. The thickness of the iron increases away from the center to improve the muon identification[6].

6 The Trigger

The *BaBar* detector has two triggering systems. The Level 1 trigger is the hardware based, and is designed to have a very high efficiency. It looks at charged particle tracks, energy cuts, or a large transverse momentum. The Level 3 trigger (software based) contains a combination of tools used to reduce backgrounds while keeping all the important events[6].

CHAPTER III

BABAR SOFTWARE

The *BaBar* experiment has very large computing requirements. It needs data acquisition, detector control, data storage, physics analysis, simulation production, network infrastructure, and other systems. The computer systems are divided into the online systems and the offline systems. The online system is responsible for control of the *BaBar* experiment, real time data acquisition, triggering, and filtering. The offline system is mainly used for physics analysis and simulation.

A The Online System

The online system performs monitoring and controlling of the experiment and manages data storage. The following list describe the online systems [9].

- Detector Control: The Detector Control manages and controls *BaBar* detector hardware, provides an interface between data acquisition and the detector, and records real time data.
- Run Control: The run control system is the overall control of the detector and does configuration, diagnosis and error recovery.
- Online Event Processing: The event processing system provides a near real time data analysis for rapid quality assurance.
- Online Data Flow: The data flow system configures and reads data from detector electronics, transports data, monitoring of dead time, and some Level 1 hardware triggers.

- Prompt Reconstruction: The prompt reconstruction gives a full physics reconstruction of data and outputs to be immediately available for analysis.

B The Offline Systems

The offline systems are not directly involved in *BaBar* data taking or control. They are mostly analysis and simulation packages. For this large collaboration, a Framework was created to give uniformity and standardization of code and work environment.

1 Framework

The Framework defines the interface between different levels of code in the offline systems. Each level of the Framework is interchangeable and enables the same analysis to be used on either real data or monte carlo simulations without any major changes to the code and to output processed data from one stage into the input data collection for another stage of analysis. These properties give the Framework extremely good flexibility. The Framework allows for three different processes. They include input from the database, output to one or more systems, and filtering and data processing. This system is extremely powerful to the analyst as it provides an opportunity to change significant parts of the analysis without recompiling the entire Framework. The method of code configuration saves significant computer time and coding effort to the analyst [10].

2 Modules

A module is a segment of the *BaBar* code and it provides a well defined specific service. The Framework is built of many individual modules each is able to be upgraded or revised to a newer version mostly independently of the other modules to decrease downtime. The following list describes the modules [10]:

- Standard Modules: These modules exist for general use, setup of the framework, and execution of utilities.

- Special Function Modules: The special function modules are designed for a specific task in the *BaBar* analysis computing environment. Some examples of these are filters, data output, and redirection of data to another module.

- User Modules: These modules include user written or modified analysis packages designed to work within the framework for the analyst's specific goals. These are kept independent from the standard modules.

3 Sequences and Paths

A sequence is a series of modules designed to work together in a specific order. These are designed for the set of modules under the sequence to either be enable or disable each particular module. The user has ultimate control of this to expedite his analysis of the needed modules for the execution. The modules are all written in the C++ programming language to follow the forms of the Framework.

A complete set of sequences, functions, data sets, setup options, and output options form what is called the path. The path contains all that is needed to form a complete analysis. The analysis can then be submitted to a computer farm to be completed [10].

4 Beta Analysis Package

The Beta software package provides all the basic tools to perform analysis at the *BaBar* experiment. It includes a collection of tools and programs to do reconstruction, identification, vertexing, tagging and other necessary procedures. From the base package, the user can include many tools and incorporate his own modules to form an analysis.

There are several requirements for the Beta package. It needs to be easy to

understand and operate for convenience of the operator. It must be a complete set of analyses and must be able to run on different platforms with all source data types.

The Beta analysis defines several objects within its framework. The first definition is of a Candidate. This is how the Beta package represents a hypothetical object that can be any type of particle. This Beta Candidate is used as a base class for all particles so they retain a common interface in the programming framework and they can be converted, interchanged, or replaced with different particles but they all remain a Beta Candidate class.

Another idea that the Beta package incorporates is the operator. The operator is a procedure to combine two Candidates into a final state Candidate or to take two final state Candidates and vertex them into a mother Candidate.

The Selector is a tool that sets acceptance cuts on data to exclude unsuitable ranges or include ranges deemed acceptable. The selection tools can be used in many stages of analysis and different selectors can also be used to clarify the data [10].

C Particle Identification

Particle identification that has high confidence levels is one of the strong points of the *BaBar* detector. The physics imposes strict requirements in the reconstruction of final states and the tagging of quarks in $B\bar{B}$ events. Each of the detector subsystems and the corresponding software play a major role in particle identification (PID). A short summary of the major particles and their methods for PID follow [11]:

Electron

- the energy to momentum ratio is on the order of 1 measured from the EMC
- match DIRC measurements with the EMC for consistencies
- EMC shower shapes should be consistent with a electron

- software analysis to deduce pion contamination

Proton

- dE/dx measurements discriminate protons from pions and kaons
- detected by DIRC above the kaon threshold

Muons

- expected interaction length in the IFR
- χ^2 of possible tracks

Photons

- energy deposition in EMC
- consistent with neutral track expectations

Charged Kaons

- dE/dx measured from SVT consistent with kaon hypothesis
- Cherenkov angle from DIRC
- likelihood from kaon to pion ratios

Neutral Long-Lived Kaons

- EMC or IFR reconstruction of neutral tracks
- shower shapes in EMC

CHAPTER IV

JET-FINDING SOFTWARE

A Jets

A jet is defined to be hadronic energy limited to an angular region resulting from a high energy interaction [12]. It is composed of the products of the decomposition of quarks or gluons into hadrons. Jets are either the groups of detected hadrons, called hadron-level jets, or the quarks and gluons, called parton-level jets that decayed into them. We are mostly concerned with the hadron-level jets as these are the most directly detectable in the laboratory. Jet finding software attempts to identify jets in an interaction from the list of detected particles and their trajectories. At *BaBar*, the jet finding software is called the JetFinder package and is maintained in the standard *BaBar* offline software releases [13].

The JetFinder package is a software module designed to identify hadronic jets from a list of Beta Candidates. It takes the list of final state particles as a list of Beta Candidates and recombines them using a particular algorithm to create the mother Candidates. These are further combined until a cut off value is reached ($y - cut$) and the final number of Beta Candidates is considered the initial representation of hadronic jets. Typically there are two jets, but sometimes there are three jet and four jet events.

The number of jets found in an event is important because these ratios can give rise to values for α_s, identification of $W^{\pm}$, fundamental properties of QCD, and fragmentation functions for gluons [4].

B Jet Finding Algorithm

Each specific jet algorithm used to combine Candidates into the initial state jets can give different results. The cone type algorithms use a clustering method to subdivide the event. A binary algorithm uses pairs of smallest energy-momentum particles and combines them into a mother Candidate. These are further combined until only the final clusters outside the cutoff region are left. These final clusters are considered to be jets.

The JetFinder package is modular in design and can be setup to use any jet clustering algorithm. In the case of an $e^+ - e^-$ collider used for *BaBar*, the Durham clustering procedure for calculating the metric is optimized for this system and is defined by [13]:

$$y_{ij} = \frac{2\min(E_i^2, E_j^2)(1 - \cos\theta_{ij})}{E_{cm}^2}$$

There are four common schemes for use in jet finding, but only one of these is available in the JetFinder software package. This E Scheme takes the energy-momentum four vectors in the center of mass frame and adds them to create a daughter particle, conserving energy and momentum. The other schemes are: the $E0$, which rescales the daughter particle to have zero invariant mass; the P, which conserves the total momentum but not the total energy; and the $P0$, which rescales the P scheme so that the total energy is equal to the sum of the daughter particles energies.

The jet finding procedure is an iterative process and is as follows:

- transform all the particle tracks into the center of mass reference frame;
- define a parameter, $y - cut$, as the maximum distance between tracks that will be considered as daughters of the same jet;
- pair all the particles and calculate a metric (y_{ij}) defining its y-value or angular separation;

- take the smallest metric and combine the two Candidates into one mother Candidate as long as the y-cut value has not been surpassed;
- remove the two daughter particles and add the mother Candidate into the Beta Candidate list;
- repeat the metric calculation for the new list of particles and continue combining particles until no more particles can be combined that do not exceed the y-cut limit;
- the remainder Candidates are considered as the initial hadronic jets .

The JetFinder software keeps an list of particles that formed each final state jet for particle identification purposes [13].

C JetFinder Organization

The JetFinder package was written using object-oriented programming. This design technique makes the program easier to develop, maintain, reuse, and modify. The modular design gives the user the power to change a particular component of the program without the difficulty of modifying the entire program through encapsulation of program components.

JetFinder contains the files listed in Table 2.

The `JetFinder` class is the primary class, containing `the main{}` routine. It controls the operations, algorithm, and user access to information. The `JetCombiner` class controls the combining of daughter particles into the mother particle using the E scheme. It also writes to the list of daughters after combining. The `JetMetric` class is the base class for the interface of `JetFinder` and the `JetMetricManager`. It sets up the framework for the classes `JetDURHAMMetric`, `JetJADEMetric`, and `JetGENEVAMetric`. These three classes define how the metric is calculated and this is controlled by `JetMetricManager`. The `JetCrossoverValue`

TABLE 2

A list of JetFinder files.

JetFinder.cc	JetCombiner.cc
JetJet.cc	JetCrossoverValue.cc
JetFinder.hh	JetCombiner.hh
JetJet.hh	JetCrossoverValue.hh
JetDURHAMMetric.cc	JetGENEVAMetric.cc
JetJADEMetric.cc	JetMetricManager.cc
JetDURHAMMetric.hh	JetGENEVAMetric.hh
JetJADEMetric.hh	JetMetricManager.hh
JetMetric.hh	HISTORY
README	GNUmakefile

class is a simple utility to maintain the list of metrics (y_{ij}) calculated by the specific metric class used. The `JetJet` class is new to the JetFinder package and is designed to make the manipulation of particles easier. It takes a list of `BtaCandidates`, a standard *BaBar* software class, and converts them into members of the `JetJet` class. This class is designed to simplify the addition of particles into a mother particle, retain information about the combined particles and to make the jets be considered a object using object-oriented programming design.

All the other files in this package are used for record keeping of changes, program notes, and compilation and linking information [13].

D JetFinder Performance

The JetFinder package can be used in any *BaBar* analysis using the `BetaUser` framework. The framework must include the user event information as an `eventInfo` object in the form `HepAList<BtaCandidate>*`. The main part of the analysis is written into the `BetaUser` framework class `WorkBook1`.

The package was tested using Monte Carlo simulated hadron-level data. This

provided the particle list input.

1 One Jet Events

The physics of e^+e^- collisions requires at least two jets. Conservation of baryon number requires that baryons be created in pairs with opposite baryon number. This, along with the conservation of momentum, makes two the minimum number of jets that can be created in this physics setup. One jet events could be caused by beam-pipe or gas collisions. This is where a particle collides with a gas particle in the beam-pipe or strays from the beam-path and strikes the pipe. This tends to spray hadrons predominantly in one direction, contaminating the data and creates the appearance of a one jet event. Tracking inefficiencies and geometry issues can cause the detector to miss detecting particles from an event, leaving the detected particle list to appear to have only one jet. All one-jet events are excluded from analysis for these considerations [13].

2 Charged and Neutral Particles

Charged particles have a greater momentum resolution than neutrals. This is primarly caused by the SVT detecting the path of the charged tracks. An investigation testing jet finding of charged tracks versus charged and neutral tracks showed that the combination is consistently closer to the truth. The tests were done on both real data and Monte Carlo [13]. For JetFinder, both charged and neutral tracks are included for the particle list.

3 Systematic Checks of JetFinder

Several tests were performed to evaluate the systematic errors of the JetFinder package. Charged particle misidentification was tested by replacing the mass of charged particles with a heavier mass. A range of y_{cut} values were used. These tests had no effect on the analysis and no systematic errors were assigned to

charged particle misidentification [13].

To check for missed track effects, 10% of the tracks were randomly removed, then the analysis was done. For the Monte Carlo, a small change was seen as compared to actual at small values of y_{cut}. The real data showed small deviances from the uncorrupted data at the upper end of the range of y_{cut} values. A conservative error of 0.1% is assigned for these missed tracks [13].

Duplicate tracks were tested with the package. For 1% duplication, small errors were introduced, but these were all inside the potential error. 5% error gave larger corruptions from baseline data and were on the order of the potential error of the system. The last case tested was 10% track duplication and this lead to very significant errors and would produce systematic errors. The expected duplication rate was 0.1% and from this study a systematic error of 1.0% was assigned [14].

The last test was for miscalculation of the transformation from the lab frame of reference to the center of mass reference. Several tests over a range of values were done and no change was seen in either real data nor in Monte Carlo. No systematic errors were assigned.

The total systematic error within the JetFinder package is taken to be within 1.005% of the resultant value [14].

E JetGen package

The JetGen software package was originally developed to be a fast Monte Carlo simulation of the fragmentation of hadronic jets. Written in the C++ programming language, it utilizes object-oriented methods for its construction and layout. The software package is a stand-alone program written using standard libraries for use under the Linux operating system. A modified version of the JetFinder package was incorporated into the JetGen package to be the jet finding software for the JetGen package. This version of JetFinder is identical in methodology to the *BaBar* version of JetFinder, but modifications had to be made

for the use of different programming libraries. The latest version as of the writing of this paper contains additional support for visualization and display software, multiple analyses of data, and improved simulation of events. JetGen's main use is as a separate stand-alone Monte Carlo to check the validity of JetFinder's jet finding efficiencies. JetGen files are listed in Table 3.

The JetGen package can be divided into three utilities: Simulation, Display, and Analysis. Both Display and Analysis are optional to the execution of the code and are implemented with command-line options.

1 Simulation

The JetGen software package's core components are contained in the Simulation files. `jetGen.cc` is the file containing the `main()` function of this program. It sets up the base program and code functions, controls the implementation of Display and Analysis, and oversees the generation of events. `InputParser` and `TraitHolder` are two classes that handle the command-line options. The first reads command-line parameters and writes them to the second. `jetGen` checks the `TraitHolder` for specific parts to use during the initial setup of the program.

`JetGenerator`, `EnergyGenerator`, `HadronGenerator`, `AGenList`, `AGenListItem`, `AGenListIterator`, and `RandomGenerator` are used in the Monte Carlo simulation. The JetGen package can simulate two, three, or four jet events. The first part of the simulation decides the energy and number of events. Then, the energy per jet is generated. Total energy and momentum is conserved in this process. Next each jet is fragmented. A jet-cone angle is decided and all particles are generated onto this cone. A random number generator decides the particles created and then the energy-momentum of the particle is removed from the total jet energy-momentum. This is repeated until there are no more particles that can be created. Using the leftover energy and momentum that is too small to fit the short

TABLE 3

A list of JetGen files.

A4Vector.cc	EnergyGenerator.cc	JetMetric.hh
A4Vector.hh	EnergyGenerator.hh	JetMetricManager.cc
AButton.cc	EvDispDrawer.cc	JetMetricManager.hh
AButton.hh	EvDispDrawer.hh	LineSketcher.cc
ACylinder.cc	EventInfo.hh	LineSketcher.hh
ACylinder.hh	GlobalAnalysis.cc	Makefile
ADrawable.cc	GlobalAnalysis.hh	ADrawable.hh
GlobalEvent.cc	RandomGenerator.cc	AGenList.hh
GlobalEvent.hh	RandomGenerator.hh	AGenListItem.hh
HISTORY	SampleAnalysis.cc	AGenListIterator.cc
HadronGenerator.cc	SampleAnalysis.hh	
AGenListIterator.hh	HadronGenerator.hh	Sketcher.cc
AHelix.cc	HelixSketcher.cc	Sketcher.hh
AHelix.hh	HelixSketcher.hh	TraitHolder.cc
AHistogram.cc	HistoManager.cc	TraitHolder.hh
AHistogram.hh	HistoManager.hh	XCoordTransformer.cc
ALine.cc	InputParser.cc	XCoordTransformer.hh
ALine.hh	InputParser.hh	XDrawer.hh
AParticle.cc	JetAnalysis.cc	XDrawerManager.cc
AParticle.hh	JetAnalysis.hh	XDrawerManager.hh
ARotator.cc	JetCombiner.cc	XParticleDrawer.cc
ARotator.hh	XParticleDrawer.hh	AVector.cc
XPositioner.cc	AVector.hh	JetCombiner.hh
XPositioner.hh	AViewer.cc	JetCrossoverValue.cc
Xencaps.cc	AViewer.hh	JetCrossoverValue.hh
Xencaps.hh	AWindow.cc	JetDURHAMMetric.cc
Xinfo.cc	AWindow.hh	JetDURHAMMetric.hh
Xinfo.hh	AnalysisBase.cc	JetFinder.cc
JetJet.cc	AnalysisBase.hh	JetFinder.hh
JetJet.h	AnalysisManager.cc	JetGENEVAMetric.cc
CylinderSketcher.cc	AnalysisManager.hh	JetGENEVAMetric.hh
CylinderSketcher.hh	Assoc.cc	JetGenerator.cc
jetGen.cc	Assoc.hh	JetGenerator.hh
JetJADEMetric.cc	JetJADEMetric.hh	

list of generated particles, a 'last particle' is created as a photon to conserve jet energy and momentum. This simple simulation only creates protons, pions, kaons, photons, electrons, and their associated anti-particles. Some options include: vary its jet-number ratios, α_s parameter, total energy, jet width, and data smearing of tracks.

The last group of files in the Simulation group are miscellaneous files. `AVector` and `A4Vector` are library files defining classes needed by JetGen. `Makefile` is a compilation and linking control file and `HISTORY` is file containing a list of changes and versions.

2 Display

The Display is used to create one or more windows in the Linux X-windowing environment. Three display modes are shown in Figure 13. These give a visual representation of the generated tracks and the initial jets. The display can be oriented to show planar projections of each pair of axes or a three-dimensional isometric view. Table 4 gives a list of files that create windows, draw components, and control the display environment.

3 JetGen Analysis Framework

The Analysis section includes the JetFinder package, creates histograms and output data files, and performs an analysis on the simulated data. `AnalysisBase`, `AnalysisManager`, and `GlobalAnalysis` are the classes that control and define the analysis class. `JetAnalysis` and `SampleAnalysis` are two analyses. `AHistogram` and `HistoManager` control the output histograms. The main function of the Analysis part of JetGen is to provide the user a outlet to examine and test the simulated data. A list of JetFinder analysis files appears in table 5.

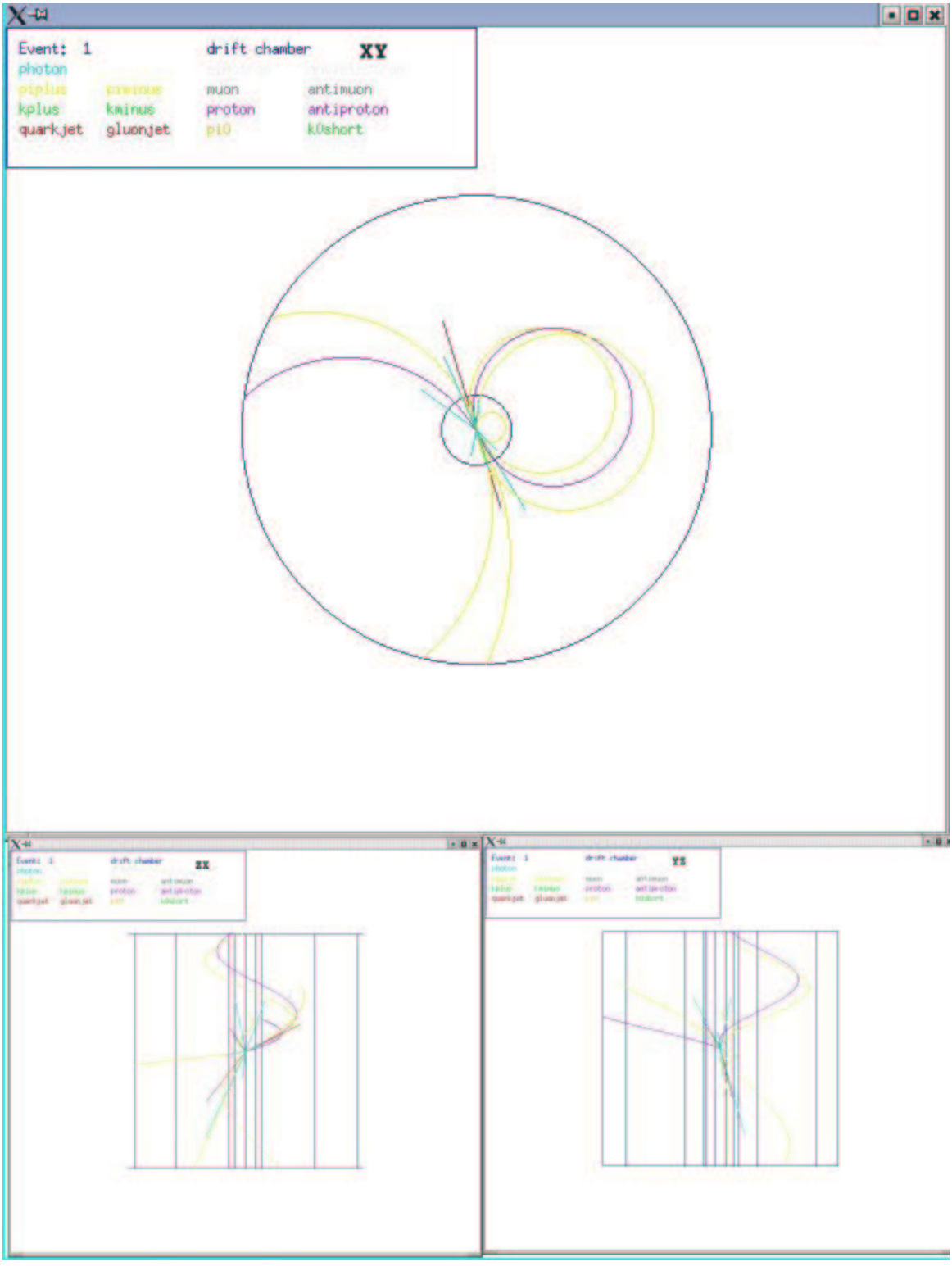

Figure 13. Three display modes of JetGen

TABLE 4

A list of JetGen files used for the display module.

EvDispDrawer.cc	EvDispDrawer.hh
LineSketcher.cc	ACylinder.cc
EventInfo.hh	LineSketcher.hh
ACylinder.hh	ADrawable.cc
ADrawable.hh	Sketcher.cc
AHelix.cc	HelixSketcher.cc
Sketcher.hh	AHelix.hh
HelixSketcher.hh	XCoordTransformer.cc
ALine.cc	XCoordTransformer.hh
ALine.hh	XDrawer.hh
XDrawerManager.cc	XDrawerManager.hh
ARotator.cc	XParticleDrawer.cc
ARotator.hh	XParticleDrawer.hh
XPositioner.cc	XPositioner.hh
AViewer.cc	Xencaps.cc
AViewer.hh	Xencaps.hh
AWindow.cc	Xinfo.cc
AWindow.hh	Xinfo.hh
CylinderSketcher.cc	CylinderSketcher.hh

TABLE 5

A list of JetGen Analysis Module files.

JetMetric.hh	JetMetricManager.cc	JetMetricManager.hh
GlobalAnalysis.cc	GlobalAnalysis.hh	SampleAnalysis.cc
SampleAnalysis.hh	AHistogram.cc	AHistogram.hh
HistoManager.hh	JetAnalysis.cc	JetAnalysis.hh
JetCombiner.cc	JetCombiner.hh	JetCrossoverValue.cc
JetCrossoverValue.hh	JetDURHAMMetric.cc	JetDURHAMMetric.hh
AnalysisBase.cc	JetFinder.cc	JetJet.cc
AnalysisBase.hh	JetFinder.hh	JetJet.h
AnalysisManager.cc	JetGENEVAMetric.cc	AnalysisManager.hh
JetGENEVAMetric.hh	JetGenerator.cc	JetGenerator.hh
JetJADEMetric.cc	JetJADEMetric.hh	

CHAPTER V

ANALYSIS

The analysis was completed using the Beta software package using the *BaBar* offline system. An analysis framework was set up to complete the tasks. The results of each were compiled into a master histogram list. Several data cuts were made, and the purified data was then processed for analysis. The output was the total numbers of particles ordered by jet energy and total numbers of protons and antiprotons ordered by jet energy. Only three jet events were examined, so the differences between quark and gluon fragmentation could be examined. The results of the total number of particles and the total number of protons were ordered by momentum. These plots were compared to give the final result. 16.5 million events were processed in 33 separate jobs. Four separate constraint mechanisms were run on these events for a total of 66 million events processed.

A Analysis Constraints

The first constraint was a particle id (PID) selection variable. One set was run under "loose" constraints. This gives more protons found, but has a higher percentage of misidentified particles, on the order of 10%. Another set was run under "tight" constraints for proton PID. This gives fewer numbers of identified protons, but has a much higher purity, over 99%. Each of these two PID constraints were run at two different y_{cut} values. The first was done within a smaller range of y_{cut} from 0.03 to 0.04. This means that the jets found have the same number of jets using both 0.03 and 0.04 as a y_{cut} for analysis. The rest were discarded. This

TABLE 6

A list of cuts done by the analysis program, numbers are approximate to its scale

Event Cut	Number	Percentage of Total
Passed all cuts	200,000	12%
no tracklist	0	0%
too few tracks	1,000,000	61%
no neutral list	0	0%
outside energy range	200,000	12%
outside momentum range	50,000	3%
charge not conserved	50,000	3%
no proton list	0	0%
y_{cut} range mismatch(2-3)	140,000	8%
y_{cut} range mismatch(3-2)	10,000	0.6%
y_{cut} range mismatch(3-4)	30	0%
jet momentum too small	0	0%

narrow metric gives less events but has a higher rate of misidentification of three jet events. The last set was done using a y_{cut} range of 0.03 to 0.08. This wider range gave a large acceptance of three jet events, but had greater errors. The four tests were done to validate the measured data and give a wide range for measurement that will allow for sampling errors in the data.

B Event Cuts

Each analysis job, totaling 132, was subject to event cuts. These cuts were instituted to increase the purity of the data, to reduce unwanted information, and to give a cleaner signal for analysis. There were twelve cuts used for this analysis. Table 6 shows these cuts.

C Measurement

The final measurement was done on antiprotons. There are significantly more protons detected than antiprotons, but conservation laws say that the number of protons and the number of antiprotons created should be the same. These extra protons come from beam-pipe events or gas interactions with the beam. A beam-pipe event is where a stray electron or positron collides with the outer beam-pipe and gives off a shower of protons. These can coincide with an e^+e^- annihilation and can be detected as part of the actual event when they did not come from the annihilation. Gas interactions are where a positron or an electron collide with one of the gas particles contained inside the beam-pipe. This will also generate a proton that may get mixed into actual data. Antiprotons were selected because they are never created in beam-pipe or gas interaction events. It can safely be said that the number of antiprotons is the same as the number of protons created in the events. This is why only the antiprotons are examined.

The number of antiprotons was counted and compared to the total number of positively charged particles. A ratio of the number of antiprotons in the lowest energy jet compared to the average of the number of antiprotons in the highest two energy jets was found. These ratios were ordered by momentum. The histgrams of each of the four analyses are displayed in Figures 14, 15, 16, and 17. Since the number of protons produced in these events is the same as the number of antiprotons produced, this ratio can be used for both.

CHAPTER VI

RESULTS

The analysis set using "loose" PID constraints and a y_{cut} range of 0.03-0.04 gave a ratio of 1.367 ± 0.030 times the number of antiprotons in jet three compared to jets one and two. Using "loose" PID and y_{cut} range of 0.03-0.08 gives a ratio of 1.343 ± 0.054. "Tight" PID and a y_{cut} range of 0.03-0.04 gives a ratio of 1.352 ± 0.030 and lastly "tight" PID and y_{cut} of 0.03-0.08 gives a ratio of 1.420 ± 0.078. A global average is $1.3705 \pm 0.0298 \pm 0.0260$ with the first error being systematic and the second statistical.

These measurements are significant because a statistical error is extremely unlikely. The measurements are 12σ from a ratio of 1:1. This is important because QCD does not predict differences in fragmentation between quark and gluon jets.

TABLE 7

Table of Results

PID type	y_{cut} range	measurement
Tight	0.03-0.04	1.352 ± 0.030
Loose	0.03-0.04	1.367 ± 0.030
Tight	0.03-0.08	1.420 ± 0.078
Loose	0.03-0.08	1.343 ± 0.054
Average		$1.3705 \pm 0.0298 \pm 0.0260$

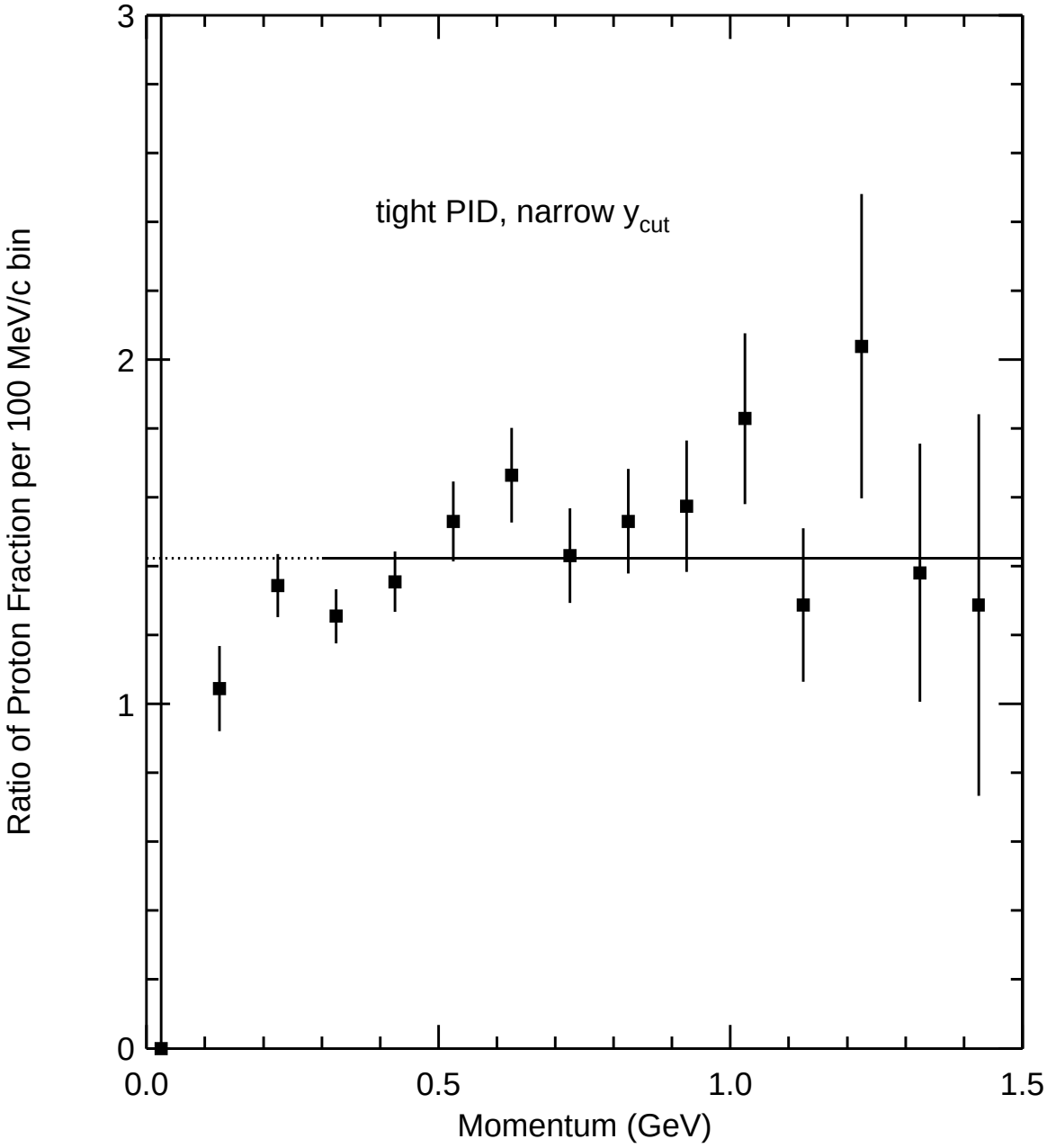

Figure 14. Ratio of antiprotons in jet 3 to antiprotons in jets 1 and 2 using tight PID and $y_{cut} 0.03 - 0.04$.

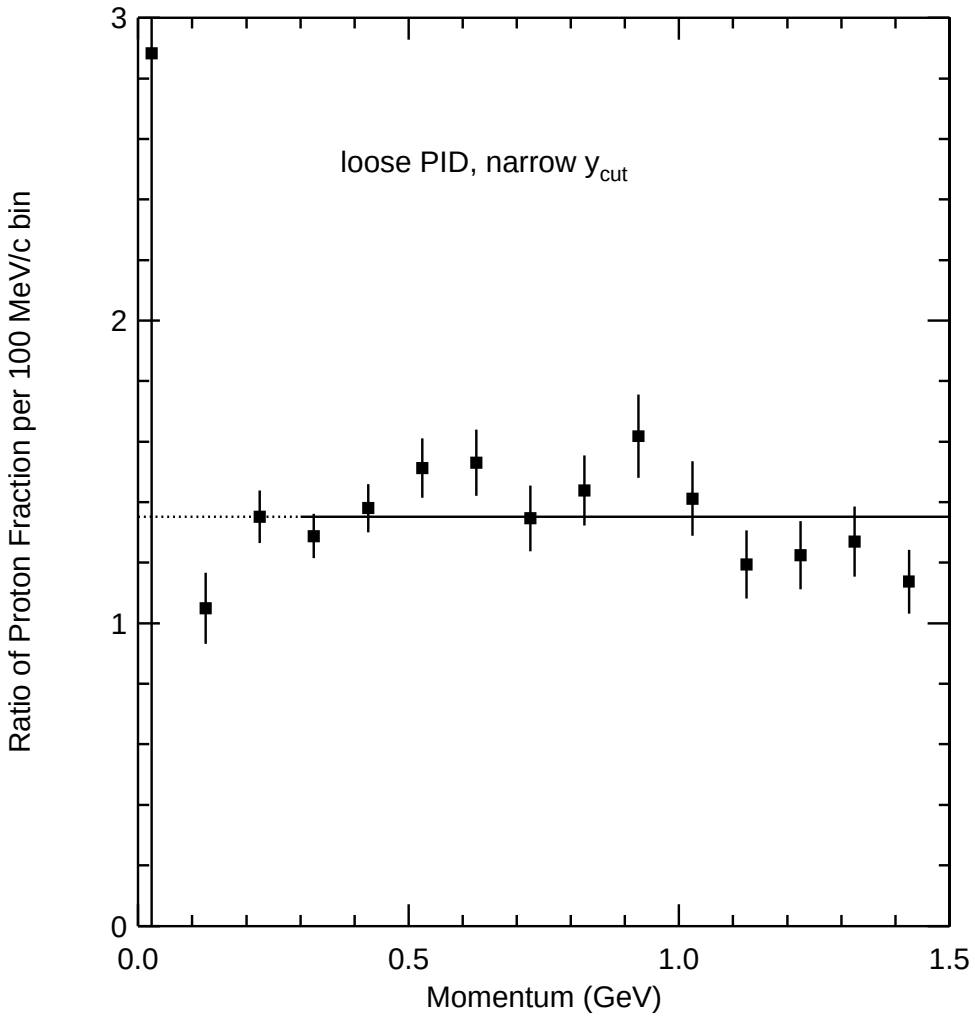

Figure 15. Ratio of antiprotons in jet 3 to antiprotons in jets 1 and 2 using loose PID and $y_{cut} 0.03 - 0.04$.

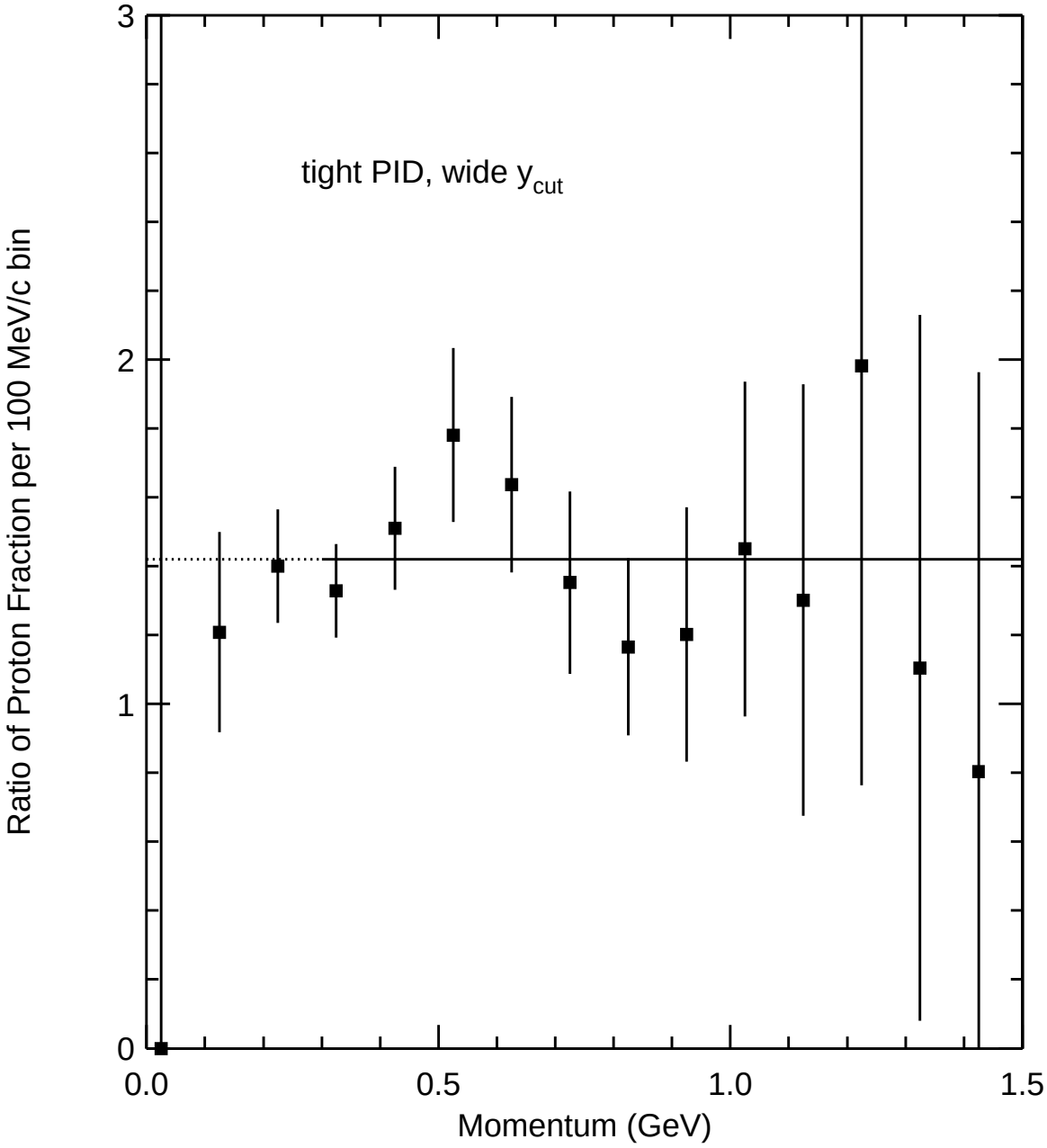

Figure 16. Ratio of antiprotons in jet 3 to antiprotons in jets 1 and 2 using tight PID and $y_{cut} 0.03 - 0.08$.

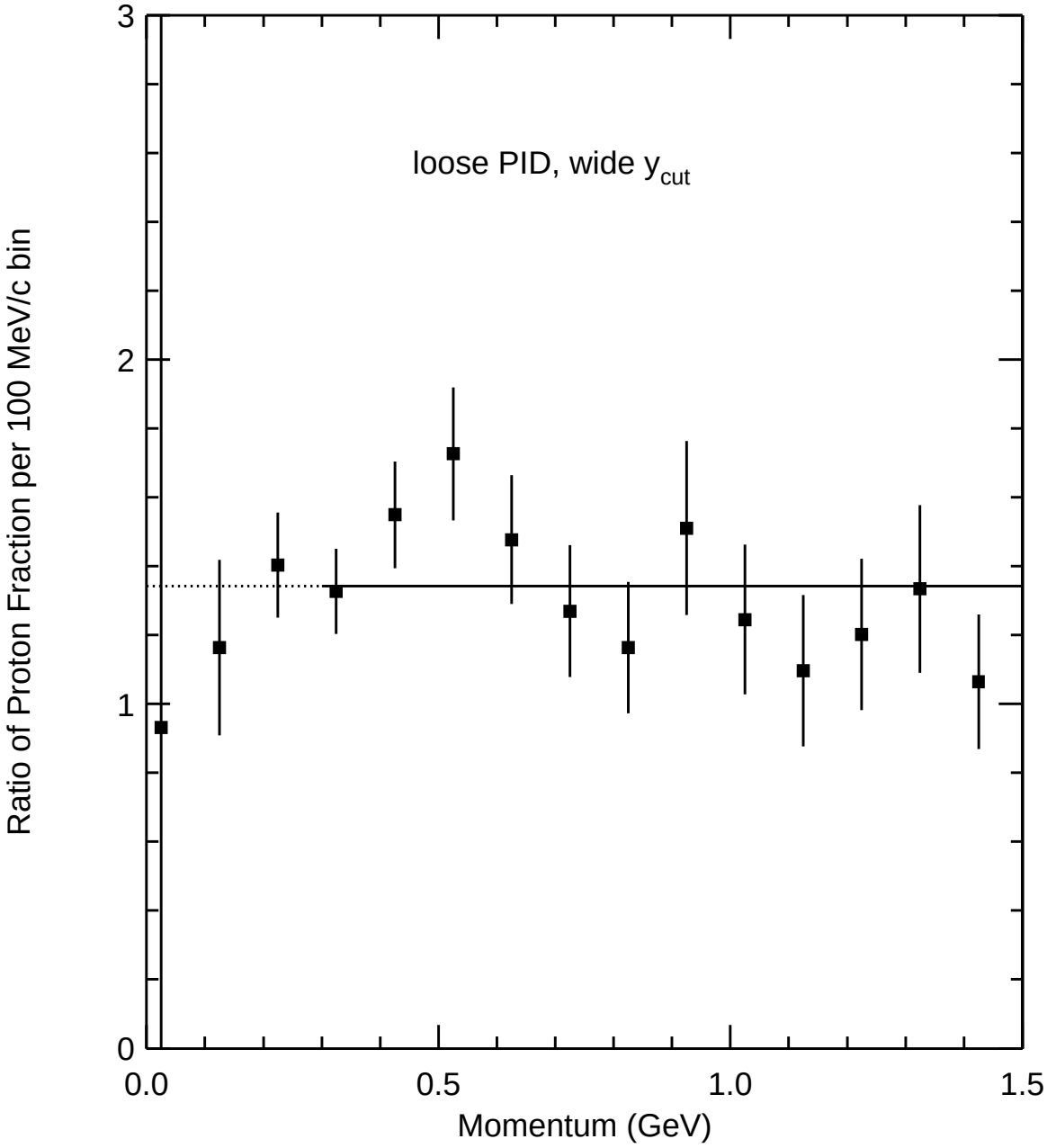

Figure 17. Ratio of antiprotons in jet 3 to antiprotons in jets 1 and 2 using loose PID and $y_{cut} 0.03 - 0.08$.

REFERENCES

[1] Donald H. Perkins *Introduction to High Energy Physics,* 4^{th} *Edition*, Cambridge University Press, 2000.

[2] Kurt Gottfried and Victor F. Weisskopf *Concepts of Particle Physics, Vol. I*, Oxford University Press, 1986.

[3] *Fermi News*, Volume 25, #2, 2002.

[4] Francis Halzen and Alan D. Martin *Quarks & Leptons: An Introductory Course in Modern Particle Physics*, Wiley Inc. 1984.

[5] David N. Brown *Inclusive Spectra in the Upsilon Energy Region and A Study of Quark-Jet Versus Gluon-Jet Fragmentation*, 1992.

[6] P. F. Harrison and H. R. Quinn, editors *The BaBar Physics Book*, 1998.

[7] http://www.slac.stanford.edu/

[8] http://www2.slac.stanford.edu/vvc/detectors.html

[9] Gregory P. Dubois-Felsmann, *The BaBar Online Computing System*, CHEP **B374**, #19, 2000.

[10] Tracy March and others, *The Workbook for BaBar Offline Users*, WWW on BaBar homepage

[11] Jian-Ping Pan *A Study of Proton Production from Quark and Gluon-Jets Near 10 GeV Center of Mass Energy*, 2002.

[12] S. Catani, *et al.* "New Clustering Algorithm for Multi-Jet Cross-sections in e^+e^- Annihilation," Phys. Lett. **B269**, 432, 1991.

[13] David N. Brown and Kelly E. Ford, "Performance of the BaBar JetFinder," *BaBar* Analysis Document #170, 2001.

[14] Kelly E. Ford *A Measurement of the Strong Coupling Constant from Jet Analysis at BaBar*, 2001.

[15] Kurt Gottfried and Victor F. Weisskopf *Concepts of Particle Physics, Vol. II*, Oxford University Press, 1986.

[16] Robert N. Cahn and Gerson Goldhaber, *The Experimental Foundations of Particle Physics*,Cambridge University Press, 1989.

[17] Joe Izen, Art Snyder, Mike Sokoloff, Roland Waldi, *Some Statistics for Particle Identification BaBar* Note **B422**, 1999.

CURRICULUM VITAE

NAME: Charles Julian Pearsall

ADDRESS: Department of Physics
University of Louisville
Louisville, KY 40292

EDUCATION: B.S. Physics
University of Louisville
2001

B.A. Music
University of Louisville
2001

PREVIOUS RESEARCH: High Energy Physics - simulations
High Energy Physics - analysis

TEACHING: Introductory Electricity and Magnetism Labs - Instructor
Introductory Electricity and Magnetism Labs - GTA
Jeffersonville High School Band Camp Instructor